Check for updates

Descriptive ecology of abyssal decapods from Chapopote Knoll (southwestern Gulf of Mexico)

Adriana Gaytán-Caballero[1], Florence Schubotz[2],
Ian R. MacDonald[3] and Elva G. Escobar-Briones[4*]

[1]Posgrado en Ciencias del Mar y Limnología, Universidad Nacional Autónoma de México, Mexico
City, Mexico, [2]MARUM - Center for Marine Environmental Sciences, University of Bremen,
Bremen, Germany, [3]Department of Earth, Ocean & Atmospheric Science, Florida State University,
Tallahassee, FL, United States, [4]Laboratorio de Biodiversidad y Macroecología, Instituto de Ciencias
del Mar y Limnología, Universidad Nacional Autónoma de México, Mexico City, Mexico

The Chapopote Knoll at 3200 m depth, in the southern Gulf of Mexico harbors highly diverse benthic habitats, including massive asphalt flows and surficial gas hydrates with gas seepage. Its associated benthic megafauna includes endemic cold-seep species and background species. This study describes the benthic habitat preferences, distribution patterns and diets of three crustacean species, the caridean shrimp *Alvinocaris muricola* and the galatheids *Munidopsis geyeri* and *M. exuta*. High-resolution imaging recorded eight habitats and helped depict their spatial distributions. *A. muricola* aggregates on Siboglinidae clusters and in gas seepage sites. *M. geyeri* and *M. exuta* are less selective and occur in almost all habitats. The carbon (δ^{13}C) and nitrogen (δ^{15}N) values of *A. muricola* show a nutritional preference of bacteria from mats and water column detritus retained among the Sibolindiae, whereas the two *Munidopsis* species have wider spectrum diets. Gut content analysis in all three species, validate the stable isotope values, food sources and confirm the secondary consumer's trophic level. This study recognizes coexistence of *A. muricola* and the two *Munidopsis* species in the benthic habitats while using different resources. Compound specific isotope analyses of galatheid guts revealed females to have more ^{13}C-depleted lipids (-35‰) compared to males (-28‰), calling for more detailed analyses to clarify this trophic segregation.

1 Introduction

The Chapopote Knoll is an asphalt volcano with diverse cold seep habitats occurring at 2914-3300 m depth (MacDonald et al., 2004; Sahling et al., 2016). Similar asphalt accumulations have been reported from other settings: Santa Barbara basin at 185-210 m depth (Valentine et al., 2010); the Angola margin asphalt mounds at 1350-2150 m depth (Jones et al., 2014); North São Paulo Plateau at 2652–2752 m depth (Fujikura et al., 2017)

and from Northern Gulf of Mexico at 975-1524 m (Puma site; Williamson et al., 2008), 1264-1365 m (Shenzi site; Weiland et al., 2008), 1150 m (Henderson site; NOAA, 2017), and 1925 m (Tar Lily sites; MacDonald, 2014). The Chapopote Knoll remains the deepest site and is distinguished by its dynamic geologic and geochemical processes that contribute to its biodiversity (Marcon et al., 2018; MacDonald et al., 2020). The chemosynthetic fauna is dominated by Siboglinidae tubeworms (*Escarpia* spp.), that occur among fissures in, or protruding from below the asphalt and authigenic carbonates crusts associated with gas hydrate mounds (MacDonald et al., 2004; Sahling et al., 2016). Modiolid bivalves (*Bathymodiolus heckerae* and *B. brooksi*) are less abundant and concentrate at methane venting soft sediment habitats (Raggi et al., 2012). Crustaceans include small peracarids that live among the Siboglinidae and on the asphalt, decapods that are dispersed over the Chapopote asphalt spill area and the neighboring background soft sediment habitat (MacDonald et al., 2004, 2020). Other fauna associated with asphalts and exposed gas hydrates includes snails, sponges, and hydroids. The microbial community is supported by the aerobic and anaerobic oxidation of hydrocarbons in association with asphalt deposits and gas hydrate (Naehr et al., 2009; Schubotz et al., 2011a, b; Raggi et al., 2012; Rubin-Blum et al., 2017; Wegener et al., 2020). The free-living microorganisms provide an important source of primary production to background and seep associated biota.

Digital images and video provide resolution to identify the faunal components and delineate their habitats. Mosaics of multiple images can increase the visual coverage obtained (Ludvigsen et al., 2007) and help understand the spatial distribution, associations among species and relationship to the cold seep habitats including potential food sources (Sibuet and Olu-Le Roy, 2002; Olu et al., 2009). These direct observations of the organisms in their ecosystem have facilitated the study of the deep-sea benthos thereby producing an integrated view of the ecosystem. The influence of fluid venting patterns and geological features define the community structure of cold seeps and dominant endemic megafauna that varies among sites (Olu et al., 2009). These criteria have been used to classify cold seeps into large field sites with conspicuous biological activity where dense clusters of endemic fauna aggregate (>1600 ind.m^{-2}); large areas with conspicuous biological activity where fauna occurs in dispersed clusters; and sites of relatively low biological activity with dispersed organisms (Sibuet and Olu-Le Roy, 2002). Carney (1994) classified the cold seep megabenthic resident community into endemic (chemosynthesis-based organisms), colonist and vagrant. The latter are background visiting fauna that benefit from the seepage microorganisms, mats and biota. Among the decapod Crustacea that occur associated to methane seepage is the caridean shrimp *Alvinocaris muricola* that has been recorded as an endemic component, and the *Munidopsis* squat lobsters referred to as colonists (Olu et al., 2009). Both species have amphi-Atlantic distribution (Komai and Segonzac, 2005; Macpherson and Segonzac, 2005; Ramirez-Llodra and Segonzac, 2006; Olu et al., 2010; Pereira et al., 2020) and coexist in the Chapopote Knoll habitats (shown in Supplementary Material). In the Regab site in the Gulf of Guinea, Komai and Segonzac (2005) described that A.

muricola feeds from protists fragments on dark mucus, and fine mineral particles. *Munidopsis geyeri*'s diet is sediment and faunal fragments as recorded by Macpherson and Segonzac (2005).

Traits associated with niche differences, presented as trade-offs among species on a local scale, include differential use of resources, susceptibility to predators, use of the abiotic environment and response to disturbance or stress (Kneitel and Chase, 2004). In particular, research of cold seep fauna diet, based on gut content, stable isotopes and fatty acids, has recorded different intake of chemosynthetic carbon and has related it to the use of the habitat in which it occurs (Olu et al., 2009; Fujikura et al., 2017). This study describes the occurrence and diet of A. muricola, M. geyeri and M. exuta on the Chapopote Knoll and contributes with new knowledge to an understanding of the interaction between species with differentiated life history and use of the cold seep habitats.

1.1 Study area

The Chapopote Knoll (meaning "tar" in Nahuatl language) is located in the Campeche Bay sub-province of the Gulf of Mexico (Figure 1A) (CONACyT, 1982). The regional bathymetry is characterized by knolls and ridges. A "craterlike graben near the crest of the structure" (MacDonald et al., 2004) characterizes the "asphalt volcano", together with the visual similarities of the asphalt discharges to *a´a* or *pa´hoehoe* basaltic lava flows (Brüning et al., 2010). This site is 5-10 km in diameter and rises 350-800 m above the surrounding lower bathyal and abyssal plain at a depth of 3000 m below sea level. The lava-like flows of solidified asphalt on Chapopote cover more than 1 km^2 of the rim. The main asphalt deposits occurred at the south-western border of the central crater-like depression (MacDonald et al., 2004; Brüning et al., 2010). Recent research on Chapopote has yielded information on the nature of asphalt seepage as a secondary result of salt tectonism, on general physicochemical features of Chapopote, and on petroleum hydrocarbon degradation (Ding et al., 2008; Brüning et al., 2010; Schubotz et al., 2011a, b; Sahling et al., 2016; Smrzka et al., 2016; Wegener et al., 2020). The bottom water that enters the Gulf of Mexico via the Caribbean Sea is North Atlantic Deep Water (NADW, 34.97‰, 4.36°C, and 5ml L^{-1}) (Vidal et al., 1994; Rivas et al., 2005) with a suggested residence time of about 250 yr (Rivas et al., 2005). The Sigsbee Abyssal Gyre (SAG) seems to be a persistent pattern of deep circulation (average speed: 5 cm s^{-1}; Pérez-Brunius et al., 2018).

2 Material and methods

The Chapopote Knoll was explored during the GeoB M67/2b cruise "Fluid seepage of Chile and in the Gulf of Mexico" on board the R/V Meteor in April 2006. In an initial phase, gas signatures in the water column, swath-mapping with the MBES Kongsberg 2040 with the AUV SEAL 5000 at an altitude of 80 m and combined with bathymetry data collected during two earlier cruises to the Campeche Knolls, and AUV surveys were used to localize active seeps and to generate high resolution bathymetric and backscatter maps. Swath
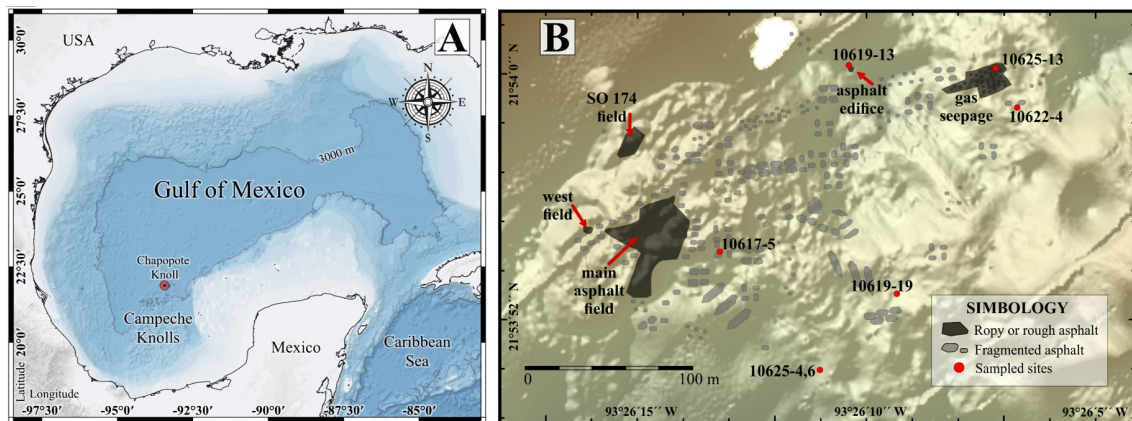
FIGURE 1
Study area and sample locations on the Chapopote asphalt volcano. **(A)** The Gulf of Mexico (base map from UNINMAR, 2011), **(B)** Insert of the Campeche Knolls within the Southwestern sector (modified from Brüning et al., 2010; Sahling et al., 2016).

mapping generates a two-dimensional area or map of the seafloor resulting from a deep- water multibeam echosounder that provide information on water depth, the roughness and smoothness of the sea floor. Areas of interest were explored with the ROV QUEST that provided the video and high-resolution images from the sea floor, assisted with the collection of organisms with scavenger traps and suction sampler (Table 1; Figure 1B).

2.1 Habitat description: image and mosaic analysis

The video recorded by the ROV was converted into a continuous image mosaic with the programs Adobe Premiere Pro, Adelie GIS (Arc View) and Adelie Video (VCR remote controller). This method is not replicable with new higher resolution strategies used but can complement those used in the Campeche Knolls. The Chapopote habitats recognized in 500 m^2 were named following the terminology and geological classification of Brüning et al. (2010) and Fink and Fletcher (1978) and compared to other cold seep sites (Sibuet and Olu-Le Roy, 2002; Ondréas et al., 2005) standardizing the habitat terminology.

2.2 Spatial distribution

The abundance of *A. muricola*, *M. geyeri* and *M. exuta* was estimated from the video images and the mosaics. The species *M. geyeri* and *M. exuta* were subsumed into *Munidopsis* spp. due to the limitations imposed by the scale of the images and impossibility to identify the two species. The relative species abundance (total number of individuals divided by the number of analyzed images in an area of 500 m^2 were reported as mean values (μ) and the ratio of variance (s^2). The species spatial distribution was classified in the two-dimensional space and named as random ($\mu=s^2$), uniform ($\mu>s^2$) and aggregated or clustered ($\mu<s^2$) (Zar, 2010). The

Correspondence Analysis (CA) was used to test the affinity of species to each habitat (Legendre and Legendre, 1998), and computed using the 'FactorMineR' library on the R statistical language and RStudio (R Core Team, 2001–2022).

2.3 Potential and ingested diet: gut content, stable isotope measurements and lipid analyses

Qualitative analysis of gut contents was based on samples observed under a stereoscopic microscope (10x magnification). The gut contents from five caridean shrimp and 17 galatheid crabs was recorded as total number of items, relative abundance, mean and standard deviation ($\mu\pm\sigma$), from smear preparations in ten subsamples prepared per sample and observed with optical microscopy. A total of 210 fields (4 cm^2 area) was observed, 50 fields in the five *A. muricola* caridean shrimps, 150 fields in the 16 *M. geyeri* and 10 fields in one *M. exuta* galatheid crabs.

The dietary preferences of the caridean shrimps and galatheid crabs were assessed in tissue and gut content by using ^{13}C/^{12}C and ^{15}N/^{14}N stable isotopic composition (Peterson and Fry, 1987). Tissue fragments were processed for elemental analysis: freeze-dried and acidified with HCl 0.1 N solution and subsequently washed with deionized water and freeze-dried before analysis, and processed in a gas chromatography (NA 2500) isotope-ratio mass spectrometer (Finnigan Delta ^{plus}XL), with values expressed in the delta notation as ‰ difference from a standard. The standard reference used for δ^{15}N was atmospheric nitrogen and the standard reference for carbon was the Vienna PeeDee Belemnite Standard with an assigned value of 0.0‰. Changes in trophic levels were identified by the 1‰ and 3.4‰ decrease from the original isotope values, for δ^{13}C and δ^{15}N, respectively (McCutchan et al., 2003).

For lipid analyses, the entire gut contents of six individuals assigned to *M. geyeri* and two *M. exuta* was solvent-extracted using a modified Bligh and Dyer method following protocols described in

TABLE 1 Sample localities and sample types.

GeoB St.	Lat N	Long W	Z (m)	Sample type
10617-5 Dive 81	21.8990	-93.4371	2919	*Munidopsis geyeri* (1), high resolution images
10619-13 Dive 82	21.8998	-93.4363	2875	High resolution images
10619-19 Dive 82	21.8987	-93.4361	2875	*Munidopsis* spp. (21), high resolution images, gut content (11 for stable isotopes, 6 from *M. geyeri* and two *M. exuta* for fatty acids), and abdominal muscle of *Munidopsis* spp. (11)
10622-4 Dive 83	21.8998	-93.4354	2907	*Alvinocaris muricola* (9), high resolution images
10625-4,6 Dive 84	21.8984	-93.4365	2916	High resolution images
10625-13 Dive 84	21.8999	-93.4354	2916	*Munidopsis* spp. (*M. geyeri* + *M. exuta*) (6), *Alvinocaris muricola* (4), high resolution images, gut content and abdominal muscle sample of *A. muricola* (3)

For sample type, the parentheses correspond to the number of individuals; Z, depth in meters.

Sturt et al. (2004). Soft tissue samples were freeze-dried and homogenized prior to dispersion in 10 ml of a solvent mixture of DCM: MeOH:buffer (1:2:0.8; v/v) and ultrasonically extracted for 10 minutes in four steps. For the first two extraction steps, a phosphate buffer was used (pH 7.4), for the last two steps the phosphate buffer was replaced by a TCA buffer (50 g/L, pH 2). Separation of the total lipid extract into free fatty acids and intact polar lipid-bound fatty acids and monoalkyl glycerolethers (MAGE) was achieved by preparative LC-MS using an Intersil Diol column (5 um, 10 x 150 mm) after Zhu et al. (2013). Subsequently, "free" and "bound" lipids were derivatized with 2.5% methanolic HCl at 70°C for 12 hrs. yielding fatty acid methyl esters (FAMEs) and bis-(trimethylsilyl) trifluoroacetamide (BSTFA, Merck, Germany) in pyridine at 70°C for 1 h yielding trimethylsilyl-(TMS)-derivatives of alcohols and ether lipids. Analysis of FAMEs and TMS-derivatives was performed by gas chromatography (GC) coupled to mass spectrometry (MS) as described previously (Schubotz et al., 2011a). Compound-specific stable carbon isotopic compositions were measured on a ThermoFinnigan GC coupled to a ThermoFinnigan Deltaplus XP isotope ratio MS. The isotopic compositions of the TMS-derivatives were corrected for the additional methyl groups introduced during derivatization. The standard deviation of replicated analysis was <1‰. All isotopic values are reported in the delta notation (δ^{13}C PDB).

3 Results

3.1 Habitat description: image and mosaic analysis

In total, 319 images and 23 mosaics were analyzed. The Chapopote Knoll study site was represented by eight habitats (Table 2; Figure 2), describing asphalt flow features, Siboglinidae clusters, gas and hydrocarbon seepages in which biota aggregate. The Siboglinidae aggregate densities of more than 50 individuals per cluster, forming a habitat for smaller species. These conspicuous clusters are restricted to the methane seepage. Megafauna that was identified associated to the seepage includes Porifera *Hymedesmia (Stylopus) methanophila* Rubin-Blum et al.,

2019 and Acarnidae *Iophon methanophila* Rubin-Blum et al., 2019, Mollusca Bivalvia *Bathymodiolus brooksi* Gustafson et al., 1998 and *Bathymodiolus heckerae* Gustafson et al., 1998; Mollusca Gastropoda *Fucaria* Warén and Bouchet, 1993; *Provanna sculpta* Warén & Ponder, 1991 and *Provanna cf* chevalieri Warén and Bouchet, 2009; Mollusca Lepetellida *Lepetodrilus shannonae* Warén and Bouchet, 2009; Annelida Polychaeta Siboglinidae *Escarpia laminata* Jones, 1985; Malacostraca Decapoda Alvinocarididae *Alvinocaris muricola* Williams, 1988; Munidopsidae *Munidopsis exuta* Macpherson and Segonzac, 2005 and *Munidopsis geyeri* Pequegnat and Pequegnat, 1970; Echinodermata Holothuroidea *Chiridota* heheva Pawson and Vance, 2004, Ophiuroidea *Ophioctenella acies* Tyler et al., 1995; Chordata Zoarcidae *Pachycara* Zugmayer, 1911.

3.2 Spatial distribution

The analysis of 319 images recognized a total of 648 specimens of the shrimp *A. muricola* and 1594 of *Munidopsis* spp. (*M. geyeri* and *M. exuta*) galatheids (Table 3). Abundances differed significantly between the shrimp and galatheid crabs (T test: t=-6.11; df=318, p=<0.0001). *A. muricola* was recorded in five habitats, with highest abundance on the gas seepage and Siboglinidae clusters (Table 3). In habitats with isolated tube worms (e.g. continuous along the asphalt flows), *A. muricola* cling to their tubes, often near the tube opening. Abundance differed between habitats (ANOVA $F_{(7,311)}$=25.85, p<0.001, n=319). In general *A. muricola* showed an aggregated distribution (26.02<1,731.33; μ<s^2).

The *Munidopsis* group (*M. geyeri* and *M. exuta*) was recorded in all eight habitats, abundance differed among habitats being highest on the continuous and ropy asphalt flow habitats (ANOVA $F_{(7,311)}$=7.53, p<0.001, n=319). The *Munidopsis* group (*M. geyeri* and *M. exuta*) also showed an aggregated distribution (8.07<66.20; μ<s^2). Correspondence analysis placed the two genera on the habitat centroids (Figure 3) and supports a dependence on variables (X^2 = 30.1685; p=0.0072) showing the association between *A. muricola* and habitats with Siboglinidae clusters and gas seepage, whereas the *Munidopsis* group (*M. geyeri* and *M. exuta*) was closely associated with the continuous and ropy asphalt flows, and the breccia habitats (Figure 3).

TABLE 2 Habitats from Chapopote knoll follow Fig. 2 (a to h).

Habitat	Asphalt deposits	Spatial location	Fauna
a) Continuous asphalt flow: Asphalt flow, fresh-ductile continuous	Heavy petroleum seepage. Relatively fresh deposit (unit 3, 4 and 5). Continuous spreading (flow), nearly smooth, as massive curves, domes or stacked pattern of flows. Scarce thin folds. Occasionally with extrusions of heavy petroleum. Analog to the smooth *pahoehoe* lava. Without sediment coverture.	Larger extensions on the "main asphalt field" (MAF), "west field" (WF), "SO174 field" (SF) (Figures 1B, 2Aa, Ba).	Characteristic biota: bacterial mats, small to meter-wide patches. Isolated *Escarpia laminata* below the asphalt flow at base (exposed tubes generally ~20cm). *Chiridota heheva* and *Alvinocaris muricola* usually on the bacterial mats, as well as *Munidopsis geyeri* and *M. exuta*.
b) Ropy asphalt flow: Asphalt flow, fresh-ropy surface	Heavy petroleum seepage. Relatively fresh deposit (unit 3 and 4). Asphalt with ropy like structures, curving, tubular, and parallel and close together folds. Analog to the ropy *pahoehoe* lava, which display extensions (parallel to the flow direction), and compressional forces at the lobe with ropes (perpendicular to the flow movement). Without sediment coverture.	Larger extensions on the "main asphalt field" (MAF), "west field" (WF), "SO174 field" (SF) as extended flows (Figures 1B, 2b-1). Flow as asphalt edifice (2m long and 1m high (Figures 1B, 2Ab-1, Bb-2).	Characteristic biota: bacterial mats (*Beggiatoa* spp.) and *Chiridota heheva* on concave surfaces or cavities between ropes formations. *Escarpia laminata* scattered below the asphalt flow at base. Clusters of ~15-20 individuals generally bearing epibionts (anemone). Caridean shrimp *A. muricola* on the tubes. *M. geyeri* and *M. exuta* in the surrounding.
c) Rough asphalt flow: Asphalt flow, rough surface	Combination of altered deposit with very-heavy petroleum seepage. Relatively old and altered deposit (unit 2). Surface irregular, anisotropic and chaotic, with fissures and cracks, which could be assigned to the shrinkage by the loss of volatile asphalt compounds, chemical oxidation, and/or biodegradation. Analog to the ropy *a´a´ rough* lava. Without sediment coverture.	Larger extensions on the "main asphalt field" (MAF), "west field" (WF), "SO174 field" (SF) (Figure 1B). In combination with, and near ropy surfaces, and, on the edge reaching the soft sediment (Figures 2Ac, Bc).	Characteristic biota: mixture of endemic and vagrant biota. Small microbial patches. Sporadic and patchy clusters (<30 ind.) of *Escarpia laminata* below the asphalt at base. *M. geyeri* and *M. exuta* scattered, as well as sea stars and hydroids.
d) Breccia: Breccia with chemosynthetic influence	Combination of altered old deposits with recent hydrocarbon seepage. Altered asphalt on breccia disposition, which is potentially formed by the recent fragmentation of asphalt deposits. Wide extensions and/or broken-apart, pieces of asphalt partly covered by soft sediment, arising apparent chemosynthetic influence.	Widespread in the rim and at the central depression. Between MAF and gas seepage habitat (Figures 1B, 2Ad-1, 2Ad-2, 2Bd-1, 2Bd-2).	Characteristic biota: mixed biota. Small microbial patches, small *Escarpia laminata* and *Bathymodiolus heckere* and *B. brooksi* clusters (<30 ind.). *Alvinocaris muricola*, related with Siboglinidae, and *M. geyeri* and *M. exuta*, scattered all around. Fragments of *Bathymodiolus* spp. and cf. *Abyssogena southwardae* valves.
e) Siboglinidae clusters: on asphalt -carbonated breccia	Combination of altered old asphalt deposits with carbonates crust and recent hydrocarbon seepage.	Near the gas seepage habitat (Figure 2Be).	Characteristic biota: *Escarpia laminata* clusters (>50 ind.). Generally, the tubes bearing epibionts (hydroids). *M. geyeri M. exuta*, and *A. muricola* in abundance. Fragments of *Bathymodiolus* spp. and cf. *Abyssogena southwardae* valves.
f) Gas seepage	Combination of altered old deposits with recent gas seepage. Asphalt brittle and stiff without stickiness. Elevation of altered asphalt. On base, a fissure which gas bubbles release. White gas hydrate on the fissure and on top of asphalt.	Northeast of the MAF (Figures 1B, 2Bf).	Characteristic biota: diverse and conspicuous endemic biota. From the top to the base: Dome with encrusting sponges, corals, and isolated *Escarpia laminata* with epibionts (hydroids); followed by *Fucaria* sp., *Provanna sculpta, Provanna* cf. *chevalieri* gastropods surrounding the fissure. On base, *Bathymodiolus heckere and B. brooksi* in a radius of about 10m. *Ophioctenella acies* ophiuroid and *Lepetodrilus* cf. *shannonae* gastropod, usually above valves. Fragments of *Bathymodiolus* spp. and cf. *Abyssogena southwardae* valves. All around, *Chiridota heheva, M. geyeri, M. exuta*, and *A. muricola*. Isolated *Pachycara* sp. fishes
g) Asphalt fragments: Soft sediment with isolated asphalt fragments	Heavily altered asphalt consisting of broken-apart, fragments visible under soft sediment without apparent chemosynthetic influence. Fragments can represent the oldest stages of asphalts as cobble- to pebble-size pieces.	On the central depression, around the chemosynthetic influence habitats and closer from the breccia habitat (Figures 2Ag, Bg).	Characteristic biota: "Lebensspuren" similar to Holothuroidea tracks.
h) Hydrocarbon seepage on soft sediment	Hemipelagic sediment with hydrocarbon seepage.	Close vicinity to the asphalt deposits (Figure 2h).	Characteristic biota: cf. *Abyssogena southwardae* and microbial patches. Anemone and *Munidopsis* one of the two species recorded (*M. geyeri* or *M. exuta*).

Brüning et al., 2010 for geophysical description of asphalt deposits and the temporal sequence in geological unities proposed. Ondréas et al., 2005; Sibuet and Olu-Le Roy, 2002, for biotic features. Complemented from Gaytán-Caballero et al., 2015; MacDonald et al., 2020; Raggi et al., 2012; Velázquez Luna, 2009, for characteristic fauna at specific level.
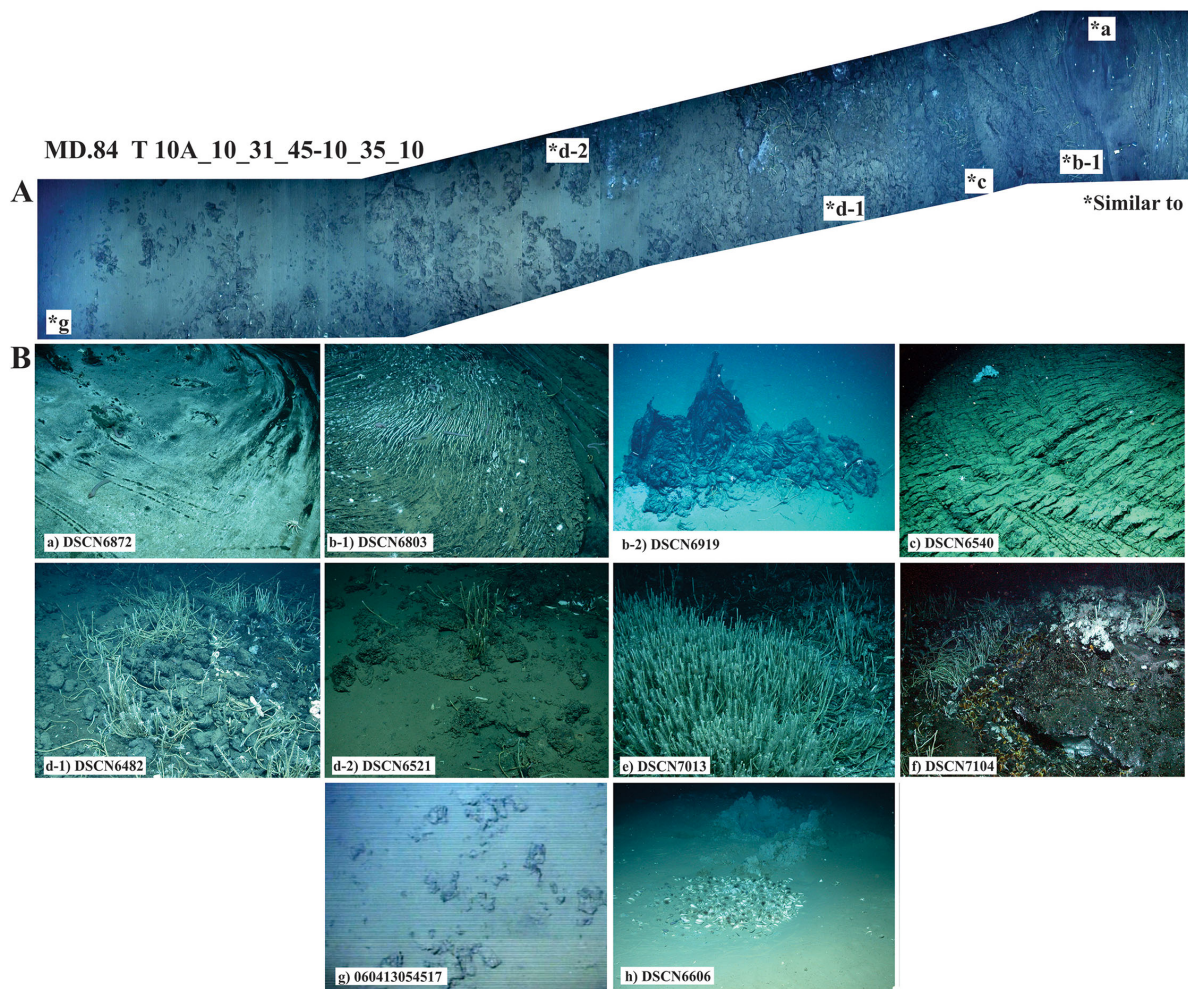
FIGURE 2
Habitats recognized on the Chapopote asphalt volcano. **(A)** mosaic showing the proximity of five different habitats. **(B)** a) Continuous asphalt flow, b-1) Ropy asphalt flow and b-2) as edifice, c) Rough asphalt flow, d-1) Breccia (less sediment covering), d-2) Breccia (more sediment covering), e) Siboglinidae clusters, f) Gas seepage, g) Asphalt fragments, h) Hydrocarbon seepage on soft sediment. "MD.84 T10A_10_31_45-10_35_10" number corresponds to video identification; DSCN= Digital Still Camera − Nikon, this is followed by the sequential number that identifies the image in the cruise and dive. All photos MARUM Copyright.

3.3 Potential and ingested diet: gut content, stable isotope, and lipid analyses

The gut content in all three species recognized twelve types of items (Figure 4). The gut contents included detritus (light brown, brown and black Figures 4A–C), filamentous material (Figure 4D), foraminifera (Figure 4E), phytodetritus (Figure 4F), diatoms (Figure 4G) and sponge ectodermal tylotes type spicules (Figure 4H). Crustacean fragments (Figure 4I) and nematodes (Figure 4J) were recognized exclusively in galatheids. Annelids (Figure 4K) and soft-walled foraminifera (Figure 4L) occurred in *M. geyeri* but were not registered in *M. exuta*.

Detritus aggregates were the most abundant item. The objects recorded in the total of sample preparations reviewed on optical microscope include brown detritus aggregates with relative

TABLE 3 Abundances of *A. muricola* and *Munidopsis* spp. (*M. geyeri* + *M. exuta*), values reported as mean and standard deviation (μ ±σ); higher values in bold.

Specie	a n=46	b n=76	c n=49	d n=26	e n=71	f n=11	g n=38	h n=2
A. muricola	0	8 (0.11 ± 0.58)	1 (0.02 ± 0.14)	37 (1.42 ± 2.63)	**473** (6.66 ± 7.96)	129 (11.73 ± 11.00)	0	0
Munidopsis spp. (*M. geyeri* + *M. exuta*),	397 (8.63 ± 11.92)	**481** (6.38 ± 5.78)	147 (3.00 ± 3.08)	143 (5.50 ± 3.34)	136 (1.92 ± 3.16)	123 (11.18 ± 12.06)	152 (4.00 ± 3.76)	11 (5.50 ± 0.71)

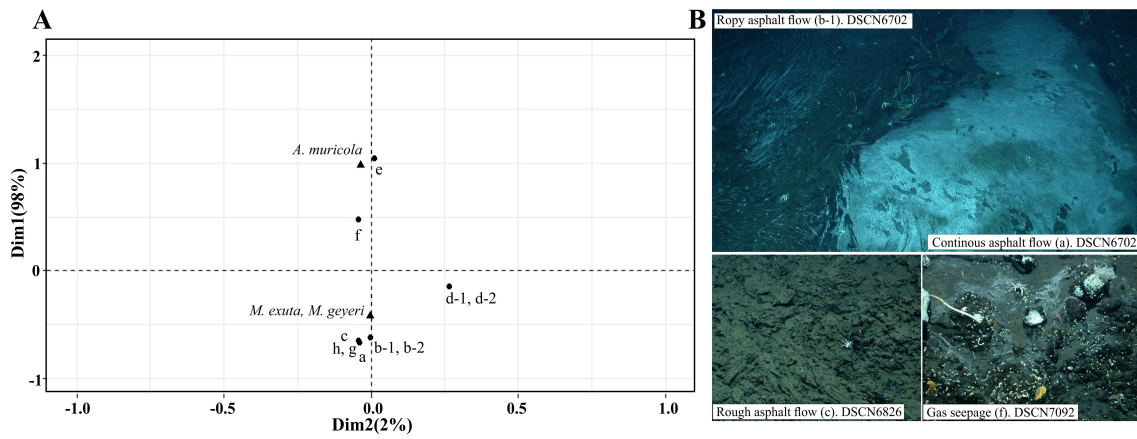n, number of replicates; a to h, habitats follow Table 2.

FIGURE 3

(A) Correspondence analysis (CA) for *A. muricola* and the two *Munidopsis* species on Chapopote, circles represent habitats: a) Continuous asphalt flow, b-1) Ropy asphalt flow and b-2) as edifice, c) Rough asphalt flow, d-1) Breccia (less sediment covering), d-2) Breccia (more sediment covering), e) Siboglinidae clusters, f) Gas seepage, g) Asphalt fragments, h) Hydrocarbon seepage on soft sediment. Markers. Circles are the benthic habitats; triangles are the species. Axes are the first two orthogonal components reproducing the distances or dimensions between the habitats and species. Dim= Dimension. **(B)** Graphic examples of distribution patterns on 4 habitats. DSCN= Digital Still Camera – Nikon, this is followed by the sequential number that identifies the image in the cruise and dive. All photos MARUM Copyright.

abundances of 18.6 ± 7.3 (μ±σ) in *A. muricola* (n=50), 34.0 ± 8.2 in *M. geyeri* (n=150), and 45 in *M. exuta* (n=10) (Figure 5). Black aggregates with 46.4 ± 4.0 in *A. muricola* (n=50), 36.3 ± 8.5 in *M. geyeri* (n=150), and 34 in *M. exuta* (n=10); and light brown aggregates with 13.2 ± 3.7 in *A. muricola* (n=50), 13.3 ± 6.6 in *M. geyeri* (n=150), and 5.8 in *M. exuta* (n=10) (Figure 5). The relative abundances of filamentous materials were 7.8 ± 2.0 in *A. muricola*, 9.4 ± 4.1 in *M. geyeri* (n=150), and 8.1 in *M. exuta* (n=10) (Figure 5). The percentage of phytodetritus in *A. muricola* (9.5 ± 3.9) was higher than in the galatheid crabs (*M. geyeri*: 1.4 ± 1.2, *M. exuta*: 1.9; Figure 5). Standard deviation data are not available for *M. exuta* as the data are from observation of 10 fields in one sample.

The bulk δ^{13}C‰ values differed between species (ANOVA F$_{(2,16)}$=8.48 p=0.003; Table 4). The carbon isotopic signature of muscle tissue for *A. muricola* had a range that included photo- and chemo-autotrophic carbon sources (-34.73 to -23.94). Depleted isotope values in the two galatheid species indicate a potential diet that includes biota from cold seeps (-41.13 to -28.25). The δ^{13}C‰ values of the gut contents in *M. exuta* were slightly enriched (Table 4, Figure 6). The δ^{15}N‰ values in muscle tissue did not differ between species (ANOVA F$_{(2,16)}$=1.04 p=0.38; Table 4), both have the same trophic level and are with a range of 6.17 ± 0.96 and 6.99 ± 1.27‰. The δ^{15}N‰ values in the gut contents of *M. geyeri* were slightly enriched.
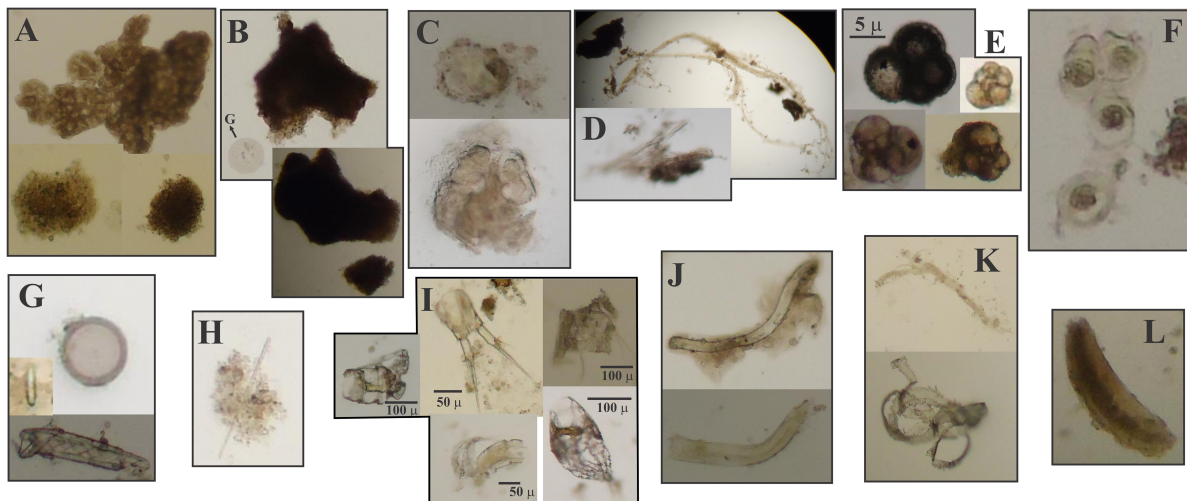

FIGURE 4

Items recorded in gut contents of *Alvinocaris muricola* and *Munidopsis* spp., optical microscopy images: Detritus (light brown, brown and black **(A–C)**, filamentous material **(D)**, foraminifera **(E)**, phytodetritus **(F)**, diatoms **(G)** and spicules **(H)**. Crustacean fragments **(I)** and nematodes **(J)**, annelids **(K)** soft-walled foraminifera **(L)**.
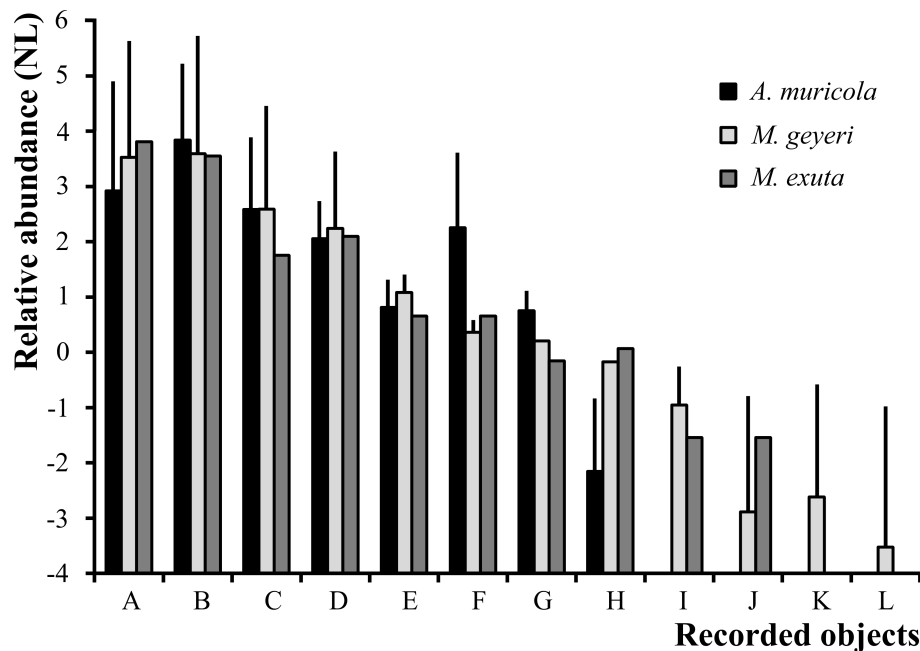
FIGURE 5
Relative abundance (Y axis: relative abundance, values in natural logarithm (NL), ln scale) of items recorded in gastric contents of *A. muricola* (*n* = 50), *M. geyeri* (*n* = 150) and *M. exuta* (*n* = 10); letters on the X-axis correspond to those of the gut content optical microscopy images detritus (light brown, brown and black **(A–C)**, filamentous material **(D)**, foraminifera **(E)**, phytodetritus **(F)**, diatoms **(G)** and spicules **(H)**. Crustacean fragments **(I)** and nematodes **(J)**, annelids **(K)** soft-walled foraminifera **(L)**. The bars are standard deviations. Standard deviation data are not available for *M. exuta* as the data are from observation of 10 fields in one sample.

Analysis of the composition and stable carbon isotopes of free fatty acids in the gut contents of *M. geyeri* (n=6) and *M. exuta* (n=2) showed low amounts of detected free fatty acids characteristic of bacteria, such as $C_{15:0}$, $C_{16:1\omega5}$, $C_{17:1}$ and cyclo-$C_{19:0}$ in the gut content. These bacterial fatty acids were often most depleted in ^{13}C (up to -58.6‰) and indicate a partly chemoautotrophic food source for female *Munidopsis* (Tables 5, 6). In contrast, male individuals contained high amounts of fatty acids enriched in ^{13}C, which can be assigned to planktonic debris, such as $C_{16:0}$, $C_{18:0}$ and $C_{20:5}$ with $\delta^{13}C$ values ranging from -27 to -24‰.

4 Discussion

4.1 Habitat description: image and mosaic analysis

Chapopote asphalt morphology varies across wide areas from fresh and ductile to old and fragmented increasing habitat heterogeneity by providing substratum for benthic biota (Jones et al., 2014). Thus, the heterogeneity of Chapopote habitats and the different types of seepage (gas and asphalt) support characteristic faunal assemblages (Table 2). Sibuet and Olu-Le Roy (2002) recognized well-defined, areas of organisms in large abundance that are clearly associated to carbonated structures. At Chapopote Knoll, we recognize two carbonated habitats: carbonate hosting Siboglinidae clusters and carbonate with breccia. Similar habitats have been observed at other chemosynthetic sites (Bergquist et al., 2003).

The megabenthic components on Chapopote are represented by families common to other described seeps sites (Ondréas et al., 2005) and contrast with other asphalt-associated ecosystems (Santa Barbara basin extinct asphalts and Angola margin asphalt mounds) where more than 50% of their biodiversity corresponds to vagrant and colonist biota (Valentine et al., 2010; Jones et al., 2014).

4.2 Spatial distribution

Both *A. muricola* and the two *Munidopsis* species displayed preference to specific habitats with an aggregated spatial distribution. In summary, Table 3 shows that *M. geyeri* and *M. exuta* occurred in all habitats in contrast with *A. muricola*. The statistical results showed patterns of occurrence in Chapopote Knoll: a larger abundance of the caridean shrimp *A. muricola* in active seepage areas which supports the biota with chemoautotrophic symbionts that provide 3D structures, *Escarpia laminata* that forms Siboglinidae clusters habitat and *Bathymodiolus heckerae - B. brooksi* mussel aggregations in the gas seeping habitat (Figure 3). These distribution patterns agree with *A. muricola* from Regab pockmark (Gulf of Guinea; Olu et al., 2009). In contrast, *Munidopsis* species had higher abundance on asphalt flows, followed by asphalt fragments and hydrocarbon seepage (Figure 3). Their presence on all habitats, as showed in mosaic of Figure 2A is similar to other deep sea background benthic species (e.g. *Echinus affinis* sea urchin and *Hyalinoecia* sp. polychaete worm; Grassle et al., 1975) that forage without preference in the diverse habitats.

TABLE 4 Isotopic signatures (δ^{13}C‰ and δ^{15}N‰), calibration standards on parenthesis.

Specie	CNCR	Sex	δ^{13}C ‰	δ^{15}N ‰	δ^{13}C ‰	δ^{15}N ‰
A. muricola	24868	♀	-34.73	6.13	($\mu\pm\sigma$)	
	24872	♀	-32.96	5.95		
	24872	♀	-23.94	5.94	-29.82 ±4.45	6.17 ± 0.96
	24873	♀	-33.12	4.77		
	24874	♂	-25.54	6.54	n=6	
	24875	–	-28.62	7.71		
M. geyeri	24845	♀	-34.15	8.46	-35.38 ±3.76	6.99 ± 1.27
	24847	♀ ov	-35.45	8.39		
	24848	♀ ov	-38.99	4.42	n=10	
	24852	♀ ov	-37.83	7.11		
	24853	♀ ov	-28.25	7.21		
	24854	♂*	-40.18	7.18		
	24859	♂	-33.88	7.07		
	24860	♂	-30.92	7.36		
	24861	♂	-38.60	5.20		
	24865	♂	-35.58	7.53		
M. exuta	24867	♀	-41.13	6.16	-40.31 ±0.74	6.82 ± 0.6
	24867	♀	-40.11	6.94		
	24869	♀	-39.70	7.35	n=3	
Gut content of *M. geyeri*	24856	♀	-32.85	2.57	-32.74 ±1.61	5.49 ± 0.66
	24847	♀ ov	-33.88	5.02		
	24847	♀ ov	-31.60	5.95	n=3	
Munidopsis spp. (*M. geyeri* + *M. exuta*) δ^{13}C‰ -36.52±3.91 (n=13) δ^{15}N‰ 6.95±1.12 (n=13)						

CNCR, identification number of deposit collection "Colección Nacional de Crustáceos, UNAM, México); n, number of replicates; ov, ovigerous; -, unidentified; *, male feminized by parasitic rhizocephalan.
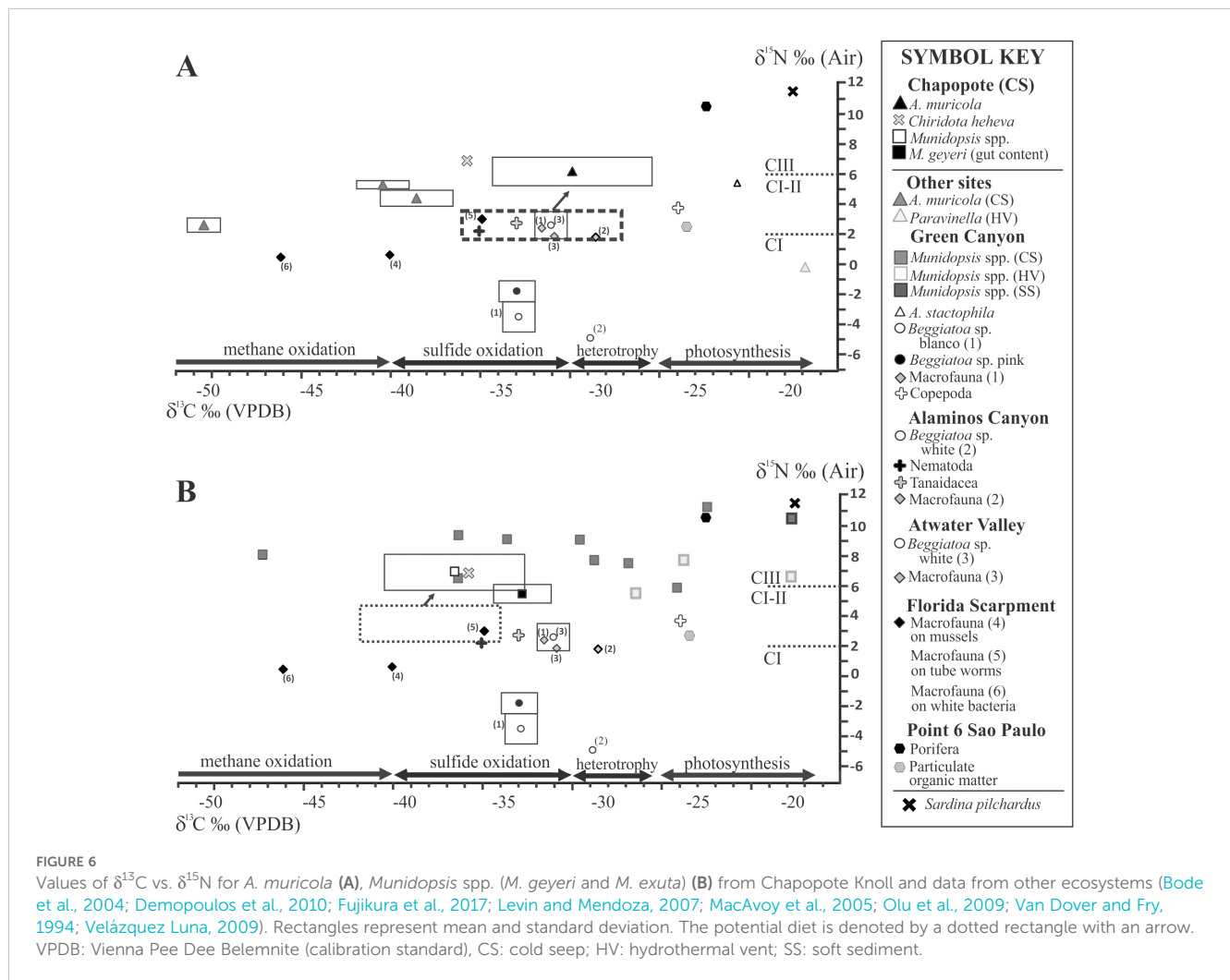
4.3 Potential and ingested diet: gut content, stable isotope measurements, and lipid analyses

A. muricola and *M. geyeri* coexist in a similar way as the analogue species that have been reported on the Regab pockmark (Olu et al., 2009). *Munidopsis exuta* is a second galatheid species that occurs on Chapopote Knoll. Although *A. muricola* showed high percentages of detritus in their gut contents, our results agree with previous reports for a similar ecosystem (Regab pockmark) (Komai and Segonzac, 2005) where their diet is chemoautotrophic-dependent in contrast with *M. geyeri* and *M. exuta* characterized by a wide-spectrum diet. We suggest a trade-off of the two taxa in differentiated life histories (Supplementary Material), where *A.*

muricola is a specialist species and *M. geyeri* and *M. exuta* are generalist organisms, able to use the resources available from diverse habitats opportunistically (MacArthur, 1972).

Muscle tissues from the three species of decapod Crustacea analyzed had δ^{13}C stable isotope values that suggest a partial chemoautotrophic carbon source (δ^{13}C ¾ -25‰; Demopoulos et al., 2010). This contrasts with fauna strongly dependent on photosynthetically fixed carbon, with enriched δ^{13}C values (-25‰ to -15‰, Fry and Sherr, 1989; -22.4 ± 0.3; Fujikura et al., 2017). The slightly enriched signal for δ^{13}C in tissues from *A. muricola* inhabiting Chapopote Knoll contrasts with previous reports from the Regab pockmark (δ^{13}C -38.5 ± 2.03 to -50.4‰ ± 0.92, n=17; Olu et al., 2009), and this supports the wide spectrum of potential food sources including chemoautotrophic organisms, detritus and/or recycled organic matter on Chapopote sediments or retained among the Siboglinidae. Related species from shallower cold seeps of the Gulf of Mexico also have enriched δ^{13}C values (e.g. -20.6‰ on *A. stactophila* at 1500 m; MacAvoy et al., 2005). In particular, *M. geyeri* had δ^{13}C depleted values, similar to those reported from the Regab pockmark (δ^{13}C -36.33 ± 1.05, n=3; Olu et al., 2009). The depleted values in *M. exuta* tissues (Table 4) as well as the presence of ^{13}C-depleted bacterial fatty acids (Tables 5, 6) reaffirm that part of the diet in *Munidopsis* is of chemoautotrophic origin in addition with other background and pelagic carbon sources. The large differences in lipid δ^{13}C values observed between individuals of one of the *Munidopsis* species (Tables 5, 6), suggest that they are highly adaptable to the available food sources, and use bacterial mats as well as water column debris. The similar δ^{15}N values recorded in all three crustacean species suggest a similar trophic position, as secondary consumers as recorded by Olu et al. (2009) for *A. muricola*: δ^{15}N 2.6 ± 0.45 to 5.3 ± 0.26‰, n=17; in the Regab pockmark. Small invertebrate and mat e.g., *Beggiatoa* sp. is potential carbon source for *A. muricola*, whereas macrofauna and meiofaunal nematodes are potential carbon sources for *Munidopsis* species. A shift in trophic position is recorded as an enrichment of δ^{13}C and δ^{15}N (Figure 6) in *A. muricola* and *Munidopsis*. Our stable isotope values lie within those recorded for similar species by Demopoulos et al. (2010) in other seep locations in the Gulf of Mexico (Figure 6) and for *M. geyeri* in the Regab pockmark (Macpherson and Segonzac, 2005; Olu et al., 2009). *Munidopsis* species seem to maintain a similar type of diet elsewhere with δ^{13}C values within the range from -1‰ to -53.30‰ in chemosynthetic ecosystems (Levin and Mendoza, 2007) and δ^{15}N values from 5.5‰ to 12.4‰ (Fisher et al., 1994; Escobar-Briones et al., 2002).

The stable carbon isotope composition of the intact polar lipid bound fatty acids and monoalkylglycerolethers, which are most likely derived from eukaryotic plasmalogens and phospholipids of the gut membrane, are very similar to the free lipids (Tables 5, 6). Females of *M. geyeri* and *M. exuta* had relatively depleted δ^{13}C in Chapopote while males had more enriched δ^{13}C lipid values (Tables 5, 6). This apparent difference, previously recorded only in albatross *Phoebastria irrorata* (Awkerman et al., 2007); skimmer bird *Rynchops niger intercedens* (Mariano-Jelicich et al., 2007); seals *Callorhinus ursinus* and rats *Rattus norvegicus* (Kurle et al., 2014) has been associated to a larger protein intake but has not been

FIGURE 6
Values of $\delta^{13}C$ vs. $\delta^{15}N$ for *A. muricola* **(A)**, *Munidopsis* spp. (*M. geyeri* and *M. exuta*) **(B)** from Chapopote Knoll and data from other ecosystems (Bode et al., 2004; Demopoulos et al., 2010; Fujikura et al., 2017; Levin and Mendoza, 2007; MacAvoy et al., 2005; Olu et al., 2009; Van Dover and Fry, 1994; Velázquez Luna, 2009). Rectangles represent mean and standard deviation. The potential diet is denoted by a dotted rectangle with an arrow. VPDB: Vienna Pee Dee Belemnite (calibration standard), CS: cold seep; HV: hydrothermal vent; SS: soft sediment.

recorded before in Crustacea. Trophic partitioning has been recorded in shrimp species (de Aquino Ferreira et al., 2022) and dietary shifts with growth have been reported in squid (Cherel et al., 2009). It will require a more detailed analysis with a larger sample set to clarify the trophic segregation recorded in males and females in the two *Munidopsis* species.

The importance of the bacterial filaments in crustacean diets has been discussed since the late 1990s (Pond et al., 1997; Polz et al., 1998). However, the nutritional role of bacterial mat or of ectobiont bacteria that grow on decapod appendices has remained enigmatic in observations made in seeps and hydrothermal vents. It is not a constant practice in all published studies to have data from direct feeding records, from experimental work, from gut content, from fatty acid and stable isotope analysis, and the presence of enzymes necessary for carbon fixation. Crustacea that potentially feed on bacterial derived carbon at chemosynthetic sites include lithodid crabs *Paralomis* sp (Niemann et al., 2013), *Shinkaia crosnieri* galatheid (Tsuchida et al., 2011; Zhao et al., 2020; Feng et al., 2023), squat lobsters *Munidopsis* spp (Zhao et al., 2020), *M. alvisca* and *M. verrilli* (Hoyoux et al., 2012), *Kiwa hirsuta* (Goffredi, 2010) and *K. puravida* crab (Thurber et al., 2011), and intermediate size shrimp *Chorocaris chacei* and adult *Rimicaris exoculata* (Gebruk et al., 2000).

Bacteria may be an important food source for seep infauna too, proving to be an essential nutritional item for seep-associated infaunal macrobenthos (Demopoulos et al., 2010). Lipid and isotope analyses provide evidence food sources (Thurber et al., 2011; Tsuchida et al., 2011), direct observation provide the behavior of feeding strategies, and specific fatty acids help trace bacterial assimilation into tissues (Pond et al., 1997). Morphological structures and tegument types are used to host, harvest or feed on bacteria. The host's behavior can benefit from a more efficient use of chemical fluxes near seeps explaining a different distribution of species using the bacteria (Feng et al., 2023).

5 Conclusions

Chapopote Knoll encompasses diverse benthic abyssal habitats. Among these the Siboglinidae clusters represent a dominant faunal component restricted to areas with methane seepage.

The decapod Crustacea species *A. muricola*, *M. geyeri* and *M. exuta* coexist spatially and feed in the asphalt volcano habitats. *A. muricola* has an aggregated distribution in the Siboglinidae clusters and gas seepage sites, and *M. geyeri* and *M. exuta* are distributed in

TABLE 5 Relative abundances and stable carbon isotope values of free fatty acids and cholesterol.

Free lipids	M. geyeri												M. exuta			
	CNCR 24845 (♀)		CNCR 24847 (♀)		CNCR 24854 (♂*)		CNCR 24855 (♀)		CNCR 24860 (♂)		CNCR 24865 (♂)		CNCR 24846 (♀ov)		CNCR 24857 (♂)	
	%	δ¹³C (‰)	%	δ¹³C (‰)	%	δ¹³C (‰)	%	δ¹³C (‰)	%	δ¹³C (‰)	%	δ¹³C (‰)	%	δ¹³C (‰)	%	δ¹³C (‰)
Fatty acids																
14:0	1	-28.5	1	-27.6	t.a.	b.d.	1	-33.0	1	-23.8	2	-24.3	t.a.	-38.2	1	-23.6
15:0	t.a.	b.d.	t.a.	-25.3	t.a.	b.d.	t.a.	-32.0	t.a.	-24.2	t.a.	-25.8	t.a.	b.d.	t.a.	b.d.
16:1ω7	7	-36.4	11	-40.0	9	-38.4	13	-37.7	7	-32.3	7	-33.0	14	-40.9	9	-35.0
16:1ω5	1	-45.2	1	-45.4	t.a.	b.d.	2	-46.4	1	-36.3	1	-44.8	1	-58.6	t.a.	b.d.
16:0	13	-32.7	14	-30.5	12	-30.2	11	-32.6	21	-26.4	21	-24.7	7	-38.3	13	-27.3
17:1	t.a.	-32.1	1	-37.5	t.a.	b.d.	1	-33.6	t.a.	b.d.	t.a.	b.d.	t.a.	b.d.	t.a.	b.d.
18:1 (ω9+ω7)	42	-35.2	35	-33.1	42	-36.8	39	-34.7	31	-25.6	31	-30.7	40	-40.1	34	-29.9
18:1	2	b.d.	2	-40.6	1	-50.6	3	-44.8	2	-36.5	2	-42.3	3	-45.1	1	-38.7
18:0	6	-34.9	5	-30.8	6	-33.2	4	-34.9	7	-26.6	7	-26.0	4	-37.9	7	-29.5
19:0 cyc	2	-40.0	1	-38.1	2	-40.6	3	-40.1	1	-29.8	1	-38.0	1	-40.0	t.a.	b.d.
20:4	t.a.	-30.5	2	-29.3	2	-29.2	3	-33.3	2	-25.4	2	-31.8	4	-33.2	4	-28.0
20:5	t.a,.	-32.7	3	-31.7	3	-29.9	5	-34.4	5	-27.0	5	-30.8	3	-34.8	6	-28.7
20:2	2	-37.7	4	-40.5	2	-27.3	5	-39.4	3	-33.8	3	-38.2	3	-41.0	t.a.	b.d.
20:1ω9	4	-35.2	6	-32.0	3	-33.7	5	-37.5	4	-25.4	4	-30.9	2	-39.1	2	-29.0
20:1ω7	8	-37.2	6	-43.0	3	-39.6	6	-41.3	3	-38.1	3	-39.7	2	-41.1	1	-36.7
22:1	1	-37.1	1	-37.8	t.a.	b.d.	1	-38.0	1	b.d.	1	-35.8	1	-39.7	2	-33.0
Cholesterol	7	-33.4	8	-32.6	15	-33.2	t.a.	-35.3	t.a.	-30.5	t.a.	-32.7	15	-34.7	20	-31.9
Weighted average	-34.2±4.1‰		-34.4±5.8‰		-35.1±6.5‰		-36.1±4.3‰		-27.2±4.9‰		-28.6±6.3‰		-39.1±5.9‰		-30.4±4.3	

CNCR, identification number of deposit collection "Colección Nacional de Crustáceos, UNAM, México), t.a., trace amounts, b.d., below detection, ♀, female, ♀ov, ovigerous female, ♂, male, ♂*, male feminized by parasitic rhizocephalan, bold, weighted average isotope values.

TABLE 6 Relative abundances and stable carbon isotope values of bound fatty acids and monoalkyl glycerol ethers (MAGE).

Bound lipids	M. geyeri												M. exuta			
	CNCR 24845 (♀)		CNCR 24847 (♀)		CNCR 24854 (♂*)		CNCR 24855 (♀)		CNCR 24860 (♂)		CNCR 24865 (♂)		CNCR 24846 (♀ov)		CNCR 24857 (♂)	
	%	δ¹³C (‰)	%	δ¹³C (‰)	%	δ¹³C (‰)	%	δ¹³C (‰)	%	δ¹³C (‰)	%	δ¹³C (‰)	%	δ¹³C (‰)	%	δ¹³C (‰)
Fatty acids																
16:1ω7	9	-28.1	14	-38.6	11	-35.1	3	-32.3	t.a.	b.d.	t.a.	b.d.	11	-34.3	t.a.	b.d.
16:0	11	-29.1	15	-30.6	23	-32.2	t.a.	-28.3	9	-19.3	34	-24.6	17	-34.2	32	-26.9
18:1(ω9+ω7)	54	-32.5	38	-34.2	47	-35.2	t.a.	b.d.	20	-24.9	t.a.	b.d.	43	-37.5	25	-29.7
18:0	5	-31.1	5	-32.8	11	-32.7	3	-29.9	8	-18.8	23	-27.3	8	-32.7	18	-28.4
20:4	3	-27.3	4	-29.2	t.a.	b.d.	t.a.	b.d.	t.a.	b.d.	t.a.	b.d.	9	-31.3	t.a.	b.d.
20:5	9	-30.6	7	-32.3	8	-30.4	t.a.	b.d.	t.a.	b.d.	t.a.	b.d.	6	-32.2	t.a.	b.d.
20:2	t.a.	b.d.	3	-37.8	t.a.	b.d.	t.a.	b.d.	t.a.	b.d.	t.a.	b.d.	t.a.	b.d.	t.a.	b.d.
20:1ω9	6	-33.7	5	-31.7	t.a.	b.d.	t.a.	b.d.	t.a.	b.d.	t.a.	b.d.	t.a.	b.d.	t.a.	b.d.
20:1ω7	t.a.	b.d.	2	-41.7	t.a.	b.d.	t.a.	b.d.	t.a.	b.d.	t.a.	b.d.	t.a.	b.d.	t.a.	b.d.
22:1	3	-32.2	t.a.	-37.8	t.a.	b.d.	t.a.	b.d.	t.a.	b.d.	t.a.	b.d.	6	-35.9	t.a.	b.d.
Monoethers																
16:0 MAGE	t.a.	b.d.	2	-38.0	t.a.	b.d.	33	-29.2	16	-29.2	43	-31.3	t.a.	b.d.	17	-29.7
18:1 MAGE	t.a.	b.d.	t.a.		t.a.	b.d.	22	b.d.	t.a.	b.d.	t.a.	b.d.	t.a.	b.d.	t.a.	b.d.
18:0 MAGE	t.a.	b.d.	t.a.	-38.4	t.a.	b.d.	20	-27.4	24	-27.4	t.a.	b.d.	t.a.	b.d.	t.a.	b.d.
20:0 MAGE	t.a.	b.d.	t.a.		t.a.	b.d.	7	-35.9	23	-35.9	t.a.	b.d.	t.a.	b.d.	t.a.	b.d.
Average	-31.4±2.2‰		-34.0±3.9‰		-33.9±2.0‰		-34.5±3.9‰		-27.8±6.4‰		-28.1±3.4‰		-35.2±2.2‰		-28.7±1.8‰	

CNCR: identification number of deposit collection "Colección Nacional de Crustáceos, UNAM, México), t.a.: trace amounts, b.d.: below detection, ♀: female, ♀ov: ovigerous female, ♂: male, ♂*: male feminized by parasitic rhizocephalan, bold: weighted average isotope values.

all habitats with a preference on asphalt flows. The diet of the three species, *A. muricola*, *M. geyeri* and *M. exuta*, with contrasting carbon sources is explained by the spatial distribution patterns.

The stable isotope composition of *A. muricola* indicates a preferential intake of chemoautotrophic organisms, detritus and/ or recycled organic matter on Chapopote sediments or retained among the Siboglinidae. In contrast the stable isotopic composition of *M. geyeri* and *M. exuta* records a wider spectrum of food items. A trophic segregation between sexes on *Munidopsis* species was recorded that will need to be verified with a larger sample set.

Data availability statement

The datasets presented in this study can be found in online repositories. The names of the repository/repositories and accession number(s) can be found in the article/Supplementary Material.

Ethics statement

The manuscript presents research on animals that do not require ethical approval for their study.

Author contributions

AG: Conceptualization, Data curation, Formal analysis, Investigation, Methodology, Visualization, Writing – review & editing. SF: Data curation, Formal analysis, Investigation, Methodology, Writing – review & editing. MI: Writing – review & editing, Conceptualization, Project administration, Resources, Validation, Visualization. EE: Conceptualization, Funding acquisition, Project administration, Resources, Validation, Visualization, Writing – review & editing, Data curation, Formal analysis, Investigation, Methodology, Software, Supervision, Writing – original draft.

Funding

Acknowledgments

Conflict of interest

The authors declare that the research was conducted in the absence of any commercial or financial relationships that could be construed as a potential conflict of interest.

The author(s) declared that they were an editorial board member of Frontiers, at the time of submission. This had no impact on the peer review process and the final decision.

Generative AI statement

The authors declare that no Gen AI was used in the creation of this manuscript.

Publisher's note

All claims expressed in this article are solely those of the authors and do not necessarily represent those of their affiliated organizations, or those of the publisher, the editors and the reviewers. Any product that may be evaluated in this article, or claim that may be made by its manufacturer, is not guaranteed or endorsed by the publisher.

Supplementary material

The Supplementary Material for this article can be found online at: https://www.frontiersin.org/articles/10.3389/fmars.2025.1534328/full#supplementary-material

References

Awkerman, J. A., Hobson, K. A., and Anderson, D. J. (2007). Isotopic (δ^{15}N and δ^{13}C) evidence for intersexual foraging differences and temporal variation in habitat use in waved albatrosses. *Can. J. Zool.* 85, 273–279. doi: 10.1139/z06-202

Bergquist, D. C., Ward, T., Cordes, E. E., McNelis, T., Howlett, S., Kosoff, R., et al. (2003). Community structure of vestimentiferan-generated habitat islands from Gulf of Mexico cold seeps. *J. Exp. Mar. Bio. Ecol.* 289, 197–222. doi: 10.1016/S0022-0981(03)00046-7

Bode, A., Álvarez-Ossorio, M. T., Carrera, P., and Lorenzo, J. (2004). Reconstruction of trophic pathways between plankton and the North Iberian sardine (*Sardina pilchardus*) using stable isotopes. *Sci. Mar.* 68, 165–178. doi: 10.3989/scimar.2004.68n1165

Brüning, M., Sahling, H., MacDonald, I. R., Ding, F., and Bohrmann, G. (2010). Origin, distribution, and alteration of asphalts at Chapopote Knoll, Southern Gulf of Mexico. *Mar. Pet. Geol.* 27, 1093–1106. doi: 10.1016/j.marpetgeo.2009.09.005

Carney, R. S. (1994). Consideration of the oasis analogy for chemosynthetic communities at Gulf of Mexico hydrocarbon vents. *Geo-Marine Lett.* 14, 149–159. doi: 10.1007/BF01203726

Cherel, Y., Fontaine, C., Jackson, G. D., Jackson, C. H., and Richard, P. (2009). Tissue, ontogenic and sex-related differences in δ^{13}C and δ^{15}N values of the oceanic squid *Todarodes filippovae* (Cephalopoda: Ommastrephidae). *Mar. Biol.* 156, 699–708. doi: 10.1007/s00227-008-1121-x

CONACyT (1982). *Ciencia y Tecnología para el aprovechamiento de los recursos marinos (situación actual, problemática y políticas indicativas)* (Mexico: Centro Cultural Universitario C.U).

de Aquino Ferreira, K., Araújo Braga, A., and Madeira Di Beneditto, A. P. (2022). Interspecific and intraspecific comparison of the isotopic niche of shrimps targets of fishing in south-eastern Brazil. *J. Mar. Biol. Assoc. United Kingdom* 102, 338–344. doi: 10.1017/S0025315422000558

Demopoulos, A. W. J., Gualtieri, D., and Kovacs, K. (2010). Food-web structure of seep sediment macrobenthos from the Gulf of Mexico. *Deep Sea Res. Part II Top. Stud. Oceanogr.* 57, 1972–1981. doi: 10.1016/j.dsr2.2010.05.011

Ding, F., Spiess, V., Brüning, M., Fekete, N., Keil, H., and Bohrmann, G. (2008). A conceptual model for hydrocarbon accumulation and seepage processes around Chapopote asphalt site, southern Gulf of Mexico: from high resolution seismic point of view. *J. Geophys. Res.* 113, 1–15. doi: 10.1029/2007JB005484

Escobar-Briones, E., Morales, P., Cienfuegos, E., and G., M. (2002). "Carbon sources and trophic position of two abyssal species of Anomura, *Munidopsis alvisca* (Galatheidae) and *Neolithodes diomedae* (Lithodidae)," in *Contributions to the Study of East Pacific Crustaceans*. Ed. M. Hendrickx (Universidad Nacional Autónoma de México, Mexico), 37–43.

Feng, W., Wang, M., Dong, D., Hui, M., Zhang, H., Fu, L., et al. (2023). Variation in epibiotic bacteria on two squat lobster species of Munidopsidae. *Front. Microbiol.* 14, 1197476. doi: 10.3389/fmicb.2023.1197476

Fink, J. H., and Fletcher, R. C. (1978). Ropy pahoehoe: surface folding of a viscous fluid. *J. Volcanol. Geotherm. Res.* 4, 151–170. doi: 10.1016/0377-0273(78)90034-3

Fisher, C. R., Childress, J. J., Macko, S. A., and Brooks, J. M. (1994). Nutritional interactions in Galapagos Rift hydrothermal vent communities: inferences from stable carbon and nitrogen isotope analyses. *Mar. Ecol. Prog. Ser.* 103, 45–55. doi: 10.3354/meps103045

Fry, B., and Sherr, E. B. (1989). "δ^{13}C Measurements as indicators of carbon flow in marine and freshwater ecosystems," in *Stable isotopes in ecological research. Ecological Studies (Analysis and Synthesis)*. Eds. P. W. Rundel, J. R. Ehleringer and K. A. Nagy (Springer, New York, NY, New York), 196–229. doi: 10.1007/978-1-4612-3498-2_12

Fujikura, K., Yamanaka, T., Sumida, P. Y. G., Bernardino, A. F., Pereira, O. S., Kanehara, T., et al. (2017). Discovery of asphalt seeps in the deep Southwest Atlantic off Brazil. *Deep Sea Res. Part II Top. Stud. Oceanogr.* 146, 35–44. doi: 10.1016/j.dsr2.2017.04.002

Gaytán-Caballero, A., MacDonald, I., Morales-Domínguez, E., and Escobar-Briones, E. (2015). "Biology," in *METEOR-Berichte, Natural hydrocarbon seepage in the southern Gulf of Mexico, Cruise No. M114. February 12 – March 28, 2015*. Eds. H. Sahling and G. Bohrmann (Editorial Assistance: DFG-Senatskommission für Ozeanographie, MARUM – Zentrum für Marine Umweltwissenschaften der Universität Bremen, Kingston (Jamaica) – Kingston (Jamaica), 39–40.

Gebruk, A. V., Southward, E. C., Kennedy, H., and Southward, A. J. (2000). Food sources, behaviour, and distribution of hydrothermal vent shrimps at the Mid-Atlantic Ridge J. *Mar. Biol. Ass. U.K.* 80, 485–499. doi: 10.1017/S0025315400002186

Goffredi, S. K. (2010). Indigenous ectosymbiotic bacteria associated with diverse hydrothermal vent invertebrates. *Environ. Microbiol. Rep.* 2, 479–488. doi: 10.1111/j.1758-2229.2010.00136.x

Grassle, J. F., Sanders, H. L., Hessler, R. R., Rowe, G. T., and McLellan, T. (1975). Pattern and zonation: a study of the bathyal megafauna using the research submersible Alvin. *Deep Sea Res. Oceanogr. Abstr.* 22, 457–481. doi: 10.1016/0011-7471(75)90020-0

Gustafson, R. G., Turner, R. D., Lutz, R. A., and Vrijenhoek, R. C. (1998). A new genus and five new species of mussels (Bivalvia: Mytilidae) from deep-sea sulfide/hydrocarbon seeps in the Gulf of Mexico. *Malacologia* 40 (1-2), 63–112. Available online at: http://biodiversitylibrary.org/page/13112012

Hoyoux, C., Zbinden, M., Samadi, S., Gaill, F., and Compère, P. (2012). Diet and gut microorganisms of Munidopsis squat lobsters associated with natural woods and mesh-enclosed substrates in the deep South Pacific. *Mar. Biol. Res.* 8, 28–47. doi: 10.1080/17451000.2011.605144

Jones, D. O. B., Walls, A., Clare, M., Fiske, M. S., Weiland, R. J., O'Brien, R., et al. (2014). Asphalt mounds and associated biota on the Angolan margin. *Deep. Res. Part I Oceanogr. Res. Pap.* 94, 124–136. doi: 10.1016/j.dsr.2014.08.010

Jones, M. L. (1985). On the Vestimentifera, new phylum: six new species, and other taxa, from hydrothermal vents and elsewhere. *Bull. Biol. Soc. Wash.* 6, 117–158.

Kneitel, J. M., and Chase, J. M. (2004). Trade-offs in community ecology: linking spatial scales and species coexistence. *Ecol. Lett.* 7, 69–80. doi: 10.1046/j.1461-0248.2003.00551.x

Komai, T., and Segonzac, M. (2005). A revision of the genus *Alvinocaris* Williams and Chace (Crustacea: Decapoda: Caridea: Alvinocarididae), with descriptions of a new genus and a new species of *Alvinocaris*. *J. Nat. Hist.* 39, 1111–1175. doi: 10.1080/00222930400002499

Kurle, C. M., Koch, P. L., Tershy, B. R., and Croll, D. A. (2014). The effects of sex, tissue type, and dietary components on stable isotope discrimination factors (δ^{13}C and δ^{15}N) in mammalian omnivores. *Isotopes Environ. Health Stud.* 50, 307–321. doi: 10.1080/10256016.2014.908872

Legendre, P., and Legendre, L. (1998). *Numerical ecology. 2nd ed* (Amsterdam: Elsevier).

Levin, L. A., and Mendoza, G. F. (2007). Community structure and nutrition of deep methane-seep macrobenthos from the North Pacific (Aleutian) Margin and the Gulf of Mexico (Florida Escarpment). *Mar. Ecol.* 28, 131–151. doi: 10.1111/j.1439-0485.2006.00131.x

Ludvigsen, M., Sortland, B., Johnsen, G., and Singh, H. (2007). Applications of georeferenced underwater photo mosaics in Marine Biology and Archaeology. *Oceanography* 20, 140–149. doi: 10.5670/oceanog.2007.14

MacArthur, R. H. (1972). *Geographical ecology: patterns in the distribution of species* (New York: Harper & Row).

MacAvoy, S. E., Fisher, C. R., Carney, R. S., and Macko, S. A. (2005). Nutritional associations among fauna at hydrocarbon seep communities in the Gulf of Mexico. *Mar. Ecol. Prog. Ser.* 292, 51–60. doi: 10.3354/meps292051

MacDonald, I. (2014). *Exploration of the Gulf of Mexico 2014: The Asphalt Ecosystem of the Gulf of Mexico* (Silver Spring: NOAA Ocean Exploration). Available at: https://oceanexplorer.noaa.gov/okeanos/explorations/ex1402/logs/apr24/apr24.html. (Accessed June 16, 2024)

MacDonald, I. R., Bohrmann, G., Escobar, E., Abegg, F., Blanchon, P., Blinova, V., et al. (2004). Asphalt volcanism and chemosynthetic life in the Campeche Knolls, Gulf of Mexico. *Science* 304, 999–1002. doi: 10.1126/science.1097154

MacDonald, I., Gaytán-Caballero, A., and Escobar Briones, E. (2020). "The asphalt ecosystem of the southern Gulf of Mexico: abyssal habitats across space and time," in *Scenarios and Responses to Future Deep Oil Spills*. Eds. S. A. Murawski, C. H. Ainsworth, S. Gilbert, D. J. Hollander, C. B. Paris, M. Schlüter and D. L. Wetzel (Cham: Springer International Publishing), 132–146. doi: 10.1007/978-3-030-12963-7_8

Macpherson, E., and Segonzac, M. (2005). Species of the genus *Munidopsis* (Crustacea, Decapoda, Galatheidae) from the deep Atlantic Ocean, including cold-seep and hydrothermal vent areas. *Zootaxa* 1095, 1–60. doi: 10.11646/zootaxa.1095.1.1

Marcon, Y., Sahling, H., MacDonald, I. R., Wintersteller, P., Ferreira, C., dos, S., et al. (2018). Slow volcanoes: The intriguing similarities between marine asphalt and basalt lavas. *Oceanography* 31, 1–12. doi: 10.5670/oceanog.2018.202

Mariano-Jelicich, R., Madrid, E., and Favero, M. (2007). Sexual dimorphism and diet segregation in the black skimmer *Rynchops Niger*. *Ardea* 95, 115–124. doi: 10.5253/078.095.0113

McCutchan, J. H. Jr., Lewis, W. M. Jr., Kendall, C., and McGrath, C. C. (2003). Variation in trophic shift for stable isotope ratios of carbon, nitrogen, and sulfur. *OIKOS* 102, 378–390. doi: 10.1034/j.1600-0706.2003.12098.x

Naehr, T. H., Birgel, D., Bohrmann, G., MacDonald, I. R., and Kasten, S. (2009). Biogeochemical controls on authigenic carbonate formation at the Chapopote "asphalt volcano", Bay of Campeche. *Chem. Geol.* 266, 390–402. doi: 10.1016/j.chemgeo.2009.07.002

Niemann, H., Linke, P., Knittel, K., MacPherson, E., Boetius, A., et al. (2013). Methane-carbon flow into the benthic food web at cold seeps – A case study from the Costa Rica subduction zone. *PloS One* 8 (10), e74894. doi: 10.1371/journal.pone.0074894

NOAA, Ocean Explorer (2017). NOAA Ship Okeanos Explorer: Gulf of Mexico 2017, Dive 09: "Henderson Ridge Mid South". Available online at: https://oceanexplorer.noaa.gov/okeanos/explorations/ex1711/dailyupdates/dailyupdates.htmlcbpi=dec11.html (Accessed January 10, 2024).

Olu, K., Caprais, J. C., Galéron, J., Causse, R., von Cosel, R., Budzinski, H., et al. (2009). Influence of seep emission on the non-symbiont-bearing fauna and vagrant species at an active giant pockmark in the Gulf of Guinea (Congo-Angola margin). *Deep. Res. Part II Top. Stud. Oceanogr.* 56, 2380–2393. doi: 10.1016/j.dsr2.2009.04.017

Olu, K., Cordes, E. E., Fisher, C. R., Brooks, J. M., Sibuet, M., and Desbruye, D. (2010). Biogeography and potential exchanges among the Atlantic Equatorial Belt cold-seep faunas. *PloS One* 5, 1–11. doi: 10.1371/journal.pone.0011967

Ondréas, H., Olu, K., Fouquet, Y., Charlou, J. L., Gay, A., Dennielou, B., et al. (2005). ROV study of a giant pockmark on the Gabon continental margin. *Geo-Marine Lett.* 25, 281–292. doi: 10.1007/s00367-005-0213-6

Pawson, D. L., and Vance, D. J. (2004). Chiridota heheva, new species, from Western Atlantic deep-sea cold seeps and anthropogenic habitats (Echinodermata: Holothuroidea: Apodida). *Zootaxa* 534, 1–12. doi: 10.11646/zootaxa.534.1

Pequegnat, L. H., and Pequegnat, W. E. (1970). "Deep-sea anomurans of superfamily Galatheoidea with description of three new species", in: *Contributions on the Biology of the Gulf of Mexico*. Eds. W. E. Pequegnat and F. A. Chace (College Station: Texas A & M University).

Pereira, O. S., Shimabukuro, M., Bernardino, A. F., and Sumida, P. Y. G. (2020). Molecular affinity of Southwest Atlantic *Alvinocaris muricola* with Atlantic Equatorial Belt populations. *Deep Sea Res. Part I Oceanogr. Res. Pap.* 163, 103343. doi: 10.1016/j.dsr.2020.103343

Pérez-Brunius, P., Furey, H., Bower, A., Hamilton, P., Candela, J., García-Carrillo, P., et al. (2018). Dominant circulation patterns of the deep Gulf of Mexico. *J. Phys. Oceanogr.* 48, 511–529. doi: 10.1175/JPO-D-17-0140.1

Peterson, B. J., and Fry, B. (1987). Stable Isotopes in ecosystem studies. *Annu. Rev. Ecol. Syst.* 18, 293–320. doi: 10.1146/annurev.es.18.110187.001453

Polz, M. F., Robinson, J. J., Cavanaugh, C. M., and Van Dover, C. L. (1998). Trophic ecology of massive shrimp aggregations at a Mid-Atlantic Ridge hydrothermal vent site. *Limnol. Oceanogr.* 43, 1631–1638. doi: 10.4319/lo.1998.43.7.1631

Pond, D. W., Dixon, D. R., Bell, M. V., Fallick, A. E., and Sargent, J. R. (1997). Occurrence on 16: 2(n-4) and 18: 2(n-4) fatty acids in the lipids of the hydrothermal vent shrimps *Rimicaris exoculata* and *Alvinocaris markensis*: nutritional and trophic implications. *Mar. Ecol. Prog. Ser.* 156, 167–174. doi: 10.3354/meps156167

Raggi, L., Schubotz, F., Hinrichs, K.-U., Dubilier, N., and Petersen, J. M. (2012). Bacterial symbionts of *Bathymodiolus* mussels and *Escarpia* tubeworms from Chapopote, an asphalt seep in the southern Gulf of Mexico. *Environ. Microbiol.* 15 (7), 1969–1987. doi: 10.1111/1462-2920.12051

Ramirez-Llodra, E., and Segonzac, M. (2006). Reproductive biology of *Alvinocaris muricola* (Decapoda: Caridea: Alvinocarididae) from cold seeps in the Congo Basin. *J. Mar. Biol. Assoc. UK* 86, 1347. doi: 10.1017/S0025315406014378

R Core Team (2001–2022). *R: a language and environment for statistical computing* (Vienna: R Found. Stat. Comput). Available at: http://www.r-project.org/ (Accessed November 10, 2023).

Rivas, D., Badan, A., and Ochoa, J. (2005). The ventilation of the deep Gulf of Mexico. *J. Phys. Oceanogr.* 35, 1763–1781. doi: 10.1175/jpo2786.1

Rubin-Blum, M., Antony, C. P., Borowski, C., Sayavedra, L., Pape, T., Sahling, H., et al. (2017). Short-chain alkanes fuel mussel and sponge *Cycloclasticus* symbionts from deep-sea gas and oil seeps. *Nat. Microbiol.* 2, 1–11. doi: 10.1038/nmicrobiol.2017.93

Rubin-Blum, M., Antony, C. P., Sayavedra, L., Martínez-Pérez, C., Birgel, D., Peckmann, J., et al. (2019). Fueled by methane: deep-sea sponges from asphalt seeps gain their nutrition from methane-oxidizing symbionts. *ISME J.* 13, 1209–1225. doi: 10.1038/s41396-019-0346-7

Sahling, H., Borowski, C., Escobar-Briones, E., Gaytán-Caballero, A., Hsu, C.-W., Loher, M., et al. (2016). Massive asphalt deposits, oil seepage, and gas venting support abundant chemosynthetic communities at the Campeche Knolls, southern Gulf of Mexico. *Biogeosciences* 13, 4491-4512. doi: 10.5194/bg-13-4491-2016

Schubotz, F., Lipp, J. S., Elvert, M., and Hinrichs, K.-U. (2011a). Stable carbon isotopic compositions of intact polar lipids reveal complex carbon flow patterns among hydrocarbon degrading microbial communities at the Chapopote asphalt volcano. *Geochim. Cosmochim. Acta* 75, 4399–4415. doi: 10.1016/j.gca.2011.05.018

Schubotz, F., Lipp, J. S., Elvert, M., Kasten, S., Mollar, X. P., Zabel, M., et al. (2011b). Petroleum degradation and associated microbial signatures at the Chapopote asphalt volcano, Southern Gulf of Mexico. *Geochim. Cosmochim. Acta* 75, 4377–4398. doi: 10.1016/j.gca.2011.05.025

Sibuet, M., and Olu-Le Roy, K. (2002). "Cold Seep communities on continental margins: structure and quantitative distribution relative to geological and fluid venting patterns," in *Ocean Margin Systems*. Eds. G. Wefer, D. Billett, D. Hebbeln, B. B. Jørgensen, M. Schlüter and T. C. E. van Weering (Springer Berlin Heidelberg, Berlin, Heidelberg), 235–225. doi: 10.1007/978-3-662-05127-6_15

Smrzka, D., Zwicker, J., Klügel, A., Monien, P., Bach, W., Bohrmann, G., et al. (2016). Establishing criteria to distinguish oil-seep from methane-seep carbonates. *Geology* 44, 667–670. doi: 10.1130/G38029.1

Sturt, H. F., Summons, R. E., Smith, K., Elvert, M., and Hinrichs, K.-U. (2004). Intact polar membrane lipids in prokaryotes and sediments deciphered by high-performance liquid chromatography/electrospray ionization multistage mass spectrometry—new biomarkers for biogeochemistry and microbial ecology. *Rapid Commun. Mass Spectrom.* 18, 617–628. doi: 10.1002/rcm.1378

Thurber, A. R., Jones, W. J., and Schnabel, K. (2011). Dancing for food in the deep sea: bacterial farming by a new species of yeti crab. *PloS One* 6, e26243. doi: 10.1371/journal.pone.0026243

Tsuchida, S., Suzuki, Y., Fujiwara, Y., Kawato, M., Uematsu, K., Yamanaka, T., et al. (2011). Epibiotic association between filamentous bacteria and the vent-associated galatheid crab, *Shinkaia crosnieri* (Decapoda: Anomura). *J. Mar. Biol. Assoc. U K* 91, 23–32. doi: 10.1017/S0025315410001827

Tyler, P. A., Paterson, G. J.L., Sibuet, M., Guille, A., Murtons, B. J., and Segonzac, M. (1995). A new genus of ophiuroid (Echinodermata: Ophiuroidea) from hydrothermal mounds along the Mid-Atlantic Ridge. *J. Mar. Biol. Ass. U.K.* 75, 977–986. doi: 10.1017/S0025315400038303

UNINMAR (2011). *Base map from Unidad de Informática Marina* (Mexico City: Instituto de Ciencias del Mar y Limnología). Available at: http://uninmar.icmyl.unam.mx/geoportal/ (Accessed July 17, 2024).

Valentine, D. L., Reddy, C. M., Farwell, C., Hill, T. M., Pizarro, O., Yoerger, D. R., et al. (2010). Asphalt volcanoes as a potential source of methane to late Pleistocene coastal waters. *Nat. Geosci.* 3, 345–348. doi: 10.1038/ngeo848

Van Dover, C. L., and Fry, B. (1994). Microorganisms as food resources at deep-sea hydrothermal vents. *Limnol. Oceanogr.* 39, 51–57. doi: 10.4319/lo.1994.39.1.0051

Velázquez Luna, R. G. (2009). *Ecología de Chiridota heheva holoturia asociada a un fondo abisal con volcanismo de asfalto en el sector Suroeste del Golfo de México* (Master Thesis, Mexico City: Universidad Nacional Autónoma de México).

Vidal, V. M. V., Vidal, F. V., Hernández, A. F., Meza, E., and Zambrano, L. (1994). Winter water mass distributions in the western Gulf of Mexico affected by a colliding anticyclonic ring. *J. Oceanogr.* 50, 559–588. doi: 10.1007/bf02235424

Warén, A., and Bouchet, P. (1993). New records, species, genera, and a new family of gastropods from hydrothermal vents and hydrocarbon seeps. *Zool. Scr.* 22, 1–90.

Warén, A., and Bouchet, P. (2009). New gastropods from deep-sea hydrocarbon seeps off West Africa. *Deep-Sea Res. II: Top. Stud. Oceanogr.* 56(23), 2326–2349. doi: 10.1016/j.dsr2.2009.04.013

Warén, A., and Ponder, W. F. (1991). New species, anatomy, and systematic position of the hydrothermal vent and hydrocarbon seep gastropod family Provannidae fam.n. (Caenogastropoda). *Zool. Scr.* 20(1), 27–56.

Wegener, G., Knittel, K., Bohrmann, G., and Schubotz, F. (2020). "Benthic deep-sea life associated with asphaltic hydrocarbon emissions in the southern Gulf of Mexico," in *Marine hydrocarbon seeps*. Eds. A. Teske and V. Carvalho (Springer, Cham), 101–123. doi: 10.1007/978-3-030-34827-4_5

Weiland, R. J., Adams, G. P., McDonald, R. D., Rooney, T. C., and Wills, L. M. (2008). "Geological and biological relationships in the Puma appraisal area: from salt diapirism to chemosynthetic communities," in *Offshore Technology Conference* (Offshore Technology Conference, Houston), 1–16. doi: 10.4043/19360-MS

Williams, A. B. (1988). New marine decapod crustaceans from waters influenced by hydrothermal discharge, brine, and hydrocarbon seepage. *Fish. Bull.* 86, 263–287.

Williamson, S. C., Zois, N., and Hewitt, A. T. (2008). "Integrated site investigation of seafloor features and associated fauna, Shenzi field, deepwater Gulf of Mexico," in *Offshore Technology Conference "Waves of Change"* (Offshore Technology Conference, Houston), 1–8. doi: 10.4043/19356-MS

Zar, J. (2010). *Biostatistical analysis. 4th ed* (Hoboken: Prentice Hall). doi: 10.1017/CBO9781107415324.004

Zhao, Y., Xu, T., Sheung Law, Y., Feng, D., Li, N., Xin, R., et al. (2020). Ecological characterization of cold-seep epifauna in the South China Sea. *Deep Sea Res Part I* 163, 103361. doi: 10.1016/j.dsr.2020.103361

Zhu, C., Lipp, J. S., Wörmer, L., Becker, K. W., Schröder, J., and Hinrichs, K.-U. (2013). Comprehensive glycerol ether lipid fingerprints through a novel reverse-phase liquid chromatography-mass spectrometry protocol. *Org. Geochem.* 65, 53–62. doi: 10.1016/j.orggeochem.2013.09.012

Zugmayer, E. (1911). Diagnoses de poissons nouveaux provenant des campagnes du yacht "Princesse-Alice" (1901 à 1910). *Bull. Inst. Océanogr. (Monaco)* 193, 1–14.